applied sciences

MDPI

Article

Utilization of Demolition Waste Enhanced with Sewage Sludge Ash and Calcium Carbide Slag for Sustainable Road Base Construction

Muhammet Çelik

Faculty of Engineering, Civil Engineering Department, Yalova University, Yalova 77200, Türkiye; muhammet.celik@yalova.edu.tr

Featured Application

This study examines the use of this waste material in road subbases by improving it with different waste materials.

Abstract

Concrete waste generated from the demolition of structures constitutes a significant source of waste worldwide. Recycled concrete aggregates (RCA) obtained from this waste exhibit disadvantages such as high porosity and low mechanical strength; therefore, they are not used in pavement structures without improvement. This study investigates the feasibility of using RCA improved with waste-based stabilizers as highway subbase material. RCA was used as fine aggregate and blended with basalt aggregate (BA) at different replacement ratios. The mixtures were subjected to California Bearing Ratio (CBR) tests to determine the optimum RCA content. Subsequently, unconfined compressive strength (UCS) tests were conducted using calcium carbide slag (CCS) as an activator and sewage sludge ash (SSA) as pozzolanic material at various proportions. The experimental results indicated that the mixture containing 35% RCA exhibited the most favorable performance, while higher RCA contents resulted in significant reduction in CBR values. The highest UCS value was obtained in the mixture containing 30% waste additive by weight of RCA with a CCS:SSA ratio of 3:7. For this mixture, CBR reached 315%, and displacement measured in the cyclic plate loading test under a load of 35 kN was 2.5 mm. This mixture provides sustainable and mechanically suitable alternatives for highway subbase applications.

Keywords: plantmix base; recycled concrete aggregate (RCA); sewage sludge ash (SSA); calcium carbide slag (CCS); sustainability

Check for updates

Received: 22 December 2025
Revised: 14 January 2026
Accepted: 14 January 2026
Published: 21 January 2026

Copyright: © 2026 by the author. Licensee MDPI, Basel, Switzerland. This article is an open access article distributed under the terms and conditions of the Creative Commons Attribution (CC BY) license.

1. Introduction

Demolition waste refers to construction materials generated during the renovation or modification of structures that have been subjected to various loads and external effects throughout their service life [1]. Large-scale demolition activities, particularly following seismic disasters, produce enormous amounts of waste debris. The 6 February 2023 Kahramanmaraş earthquakes alone resulted in 350 to 850 million tons of demolition waste [2]. Official figures released in 2023 indicate that Türkiye has 28.6 million buildings, 6.7 million (~23.4%) of which are classified as structurally risky in the event of an earthquake [3]. Consequently, earthquake-prone countries like Türkiye must undergo urgent urban renewal efforts [4]. However, this process leads to massive demolition waste disposal challenges.

Demolition waste may contain concrete blocks, bricks, lime, wood, metal, bituminous, and plastic materials. In terms of mass, 75–80% of this waste consists of concrete and brick materials [5]. A study has determined that approximately 60% of 1 m^3 of demolition waste can be recycled, while another study has reported that this rate can reach up to 90% [6]. However, unfortunately, worldwide, these wastes are not fully utilized, and a significant portion is disposed of in vacant lands [7].

The storage of demolition waste not only incurs high costs but also poses environmental risks. On the other hand, in line with the principle of sustainability, research on the reuse of demolition waste continues. The partial use of recycled concrete aggregate (RCA) instead of newly produced virgin aggregate can help reduce carbon emissions to some extent, particularly those generated during the production and transportation of aggregates extracted from quarries located far from residential areas [8,9]. Research has been conducted on the various applications of recycled concrete aggregate (RCA) in the construction sector. In particular, numerous studies in the literature have explored the use of RCA in road base and subbase construction [10–12]. A summary of some of these studies and the findings obtained is as follows.

In a study conducted by Aytekin (2023) [1], recycled concrete aggregate (RCA) was mixed with crushed limestone aggregate at ratios of 0%, 25%, 50%, 75%, and 100%. The findings indicated that some of these mixtures met the lower limit values specified in the Technical Specifications of the Turkish Republic Highways (KTŞ). However, it was also noted that RCA alone did not meet the required specification standards [1]. In another study conducted by Tabyang et al. (2022) [13], municipal solid waste ash was used to improve the strength of RCA for use in road construction. As alkali activators, liquid sodium metasilicate (Na_2SiO_3) and sodium hydroxide (NaOH) solutions were added. The study investigated the suitability of the resulting material for use as a pavement base. The findings revealed that the best results were obtained when 10% municipal solid waste ash was added [13]. In a study conducted by Arulrajah et al. (2016) [14], demolition waste consisting of bricks and concrete was stabilized for road base applications using mixtures of fly ash, blast furnace slag, and carbide sludge. The binder content in the mixtures was adjusted to 10%, and the materials were combined in binary combinations at different ratios. Additionally, an alkali activator was introduced to enhance bond formation within the mixture. The final mixture was prepared for use in road base and subbase layers. The best performance was achieved using a combination of 5% carbide sludge and 5% blast furnace slag [14]. Fly ash has also been used to improve the properties of soil layers. In their 2022 study, Chompoorat et al. found that fly ash added to cement at a rate of up to 15% met the standards required for soil reinforcement [15]. In general, RCA is reported to have low or inconsistent strength values, high porosity, and consequently high water absorption capacity and abrasion values. Due to these drawbacks, it is recommended that RCA should be reinforced with natural aggregates or other additive materials [1,13,16]. On the other hand, it is also known that the addition of materials such as cement and lime improves the properties of RCA for use in road layers [17,18]. However, the production of cement and lime releases a significant amount of carbon emissions into the environment [19,20]. Data indicates that 10% of global carbon emissions result from cement production, while 2% originate from lime production. According to these figures, the production of 1 ton of Portland cement leads to the emission of 1 ton of CO_2 into the atmosphere [12]. To summarize, as evident from the literature review, a significant volume of concrete waste is projected to be generated in the near future. Without proper planning, this waste will be disposed of in vacant areas, posing a threat to the environment. On the other hand, research and strategic planning can facilitate the reuse of RCA. Previous studies have shown that materials composed entirely of 100% RCA do not yield successful results when used alone

in road base and subbase applications [1,11,18,21,22]. At this point, it is recommended that RCA either be mixed with virgin aggregate or enhanced with different mixtures. Studies indicate that improving the properties of RCA would be beneficial for its utilization in construction applications [23,24]. Although cement and lime are commonly used materials for enhancing RCA properties, researchers are investigating alternative materials with a lower carbon footprint. At this point, various pozzolanic waste materials, such as fly ash and blast furnace slag, can be used as alternatives to cement due to their binding properties [15]. In particular, it has been found that the use of materials with high $Ca(OH)_2$ content as alkaline activators improves bonding capabilities [25]. In this study, two different waste materials (CCS, SSA) are used to improve RCA properties.

Calcium carbide sludge (CCS) is a waste byproduct generated from the hydrolysis of calcium carbide during acetylene gas production. It contains a high amount of $Ca(OH)_2$ [26] and is classified as an alkali-activated material with low carbon emissions [11]. Due to its $Ca(OH)_2$ content, CCS is known to exhibit binding properties by reacting with materials containing silicon and aluminum oxides [5,13,27]. It has been observed that, due to its binding ability, CCS enhances the strength of the materials it is mixed with while reducing their permeability [28]. Additionally, studies have shown that CCS lowers the hydration heat, thereby reducing the risk of thermal cracking. It also improves resistance to chemical deterioration caused by sulfates and chlorides [29]. The proportion of CCS added as an alkali activator in the material must be carefully considered; if added in insufficient quantities, it cannot create an adequate alkaline medium and will not provide the desired benefits. When too much is added, the strength obtained decreases, etringite formation is observed, the environment becomes excessively alkaline, which damages the C-S-H bonds, and finally, an excessive amount of unreacted calcium hydroxide remains in the environment, which reacts with CO_2 to form porous limestone, which increases permeability. Therefore, it is important that almost all of the CCS added to the mixture is consumed [30,31]. In previous studies, the ratio of CCS to binder has ranged from 10% to 40% [32–38]. CCS is generally dried in the sun or in an oven to a constant moisture content, ground, and passed through sieves with apertures of 40 or smaller. It has been determined that the lower the particle size, the more reactive it is [25,32,39]. A study conducted in 2024 determined that 28 million tons of CCS is produced worldwide annually, with approximately 55% of it being utilized [40]. Additionally, the production volume continues to increase each year [41]. On the other hand, a study in Türkiye in 2019 reported that waste CCS could not be reused and was instead transported to storage sites [42]. Globally, the unused portion of CCS in recycling is disposed of in vacant lands, causing environmental damage and leading to issues such as unpleasant odors [43]. Therefore, planning for its reuse through research is important.

In this study, sewage sludge ash (SSA) was used alongside carbide sludge to improve the properties of recycled concrete aggregate (RCA). The use of CCS together with SSA is mechanistically justified by the pozzolan–lime synergy between $Ca(OH)_2$-rich CCS and the reactive aluminosilicate phases in SSA [25,28]. In cementitious and alkali-activated systems, the amorphous silica in SSA can consume calcium hydroxide and contribute to additional C–S–H-type gel formation, while $Ca(OH)_2$-based residues provide both a highly alkaline pore solution and Ca^{2+} that promote precursor dissolution and hydrated gel precipitation. Consequently, adopting an SSA-rich blend can be theoretically rationalized as a balance that supplies sufficient $Ca(OH)_2$ for activation while maximizing reactive silica availability and minimizing unreacted $Ca(OH)_2$ [44,45]. Sewage sludge is a semi-solid/liquid material collected from wastewater treatment plants [46]. With population growth and infrastructure development worldwide, the production of municipal solid waste is expected to increase significantly, reaching 3.4 billion tons by 2050 [47]. These wastes cause various environ-

mental problems. In recent years, they have played a significant role in the formation of mucilage. Mucilage is an organic material produced by various marine organisms and negatively affects marine life due to its structure and odor [48]. A study has found that nitrogen and phosphorus in sewage waste are critical factors in the formation of mucilage, and this problem intensifies in stagnant inland seas [49]. One of the most effective solutions to this issue is waste incineration plants. In these facilities, sewage waste is converted into solid waste and then transformed into thermal energy, thus providing a sustainable benefit by generating energy while preventing the release of hard-to-recycle waste into the sea [50]. The incineration of solid waste results in the formation of three new types of waste: bottom ash, fly ash, and gas emissions. The use of bottom ash and fly ash as construction materials is an area of ongoing research. The presence of active alkalis in the ashes has further encouraged studies in this field. However, the physical and chemical properties of the ash vary depending on factors such as the facility where it is produced, the type of raw material burned, and the process used (incineration or treatment) [51].

In this study, the potential use of RCA waste, which is expected to emerge in earthquake-prone countries like Türkiye in the near future, was examined for pavement base applications in highways after an improvement process using other waste materials. As an alternative to cement and lime, the improvement process incorporated sewage sludge ash (SSA), which exhibits pozzolanic properties, and carbide sieve sludge (CCS), a waste material that is an alkaline activator with a high calcium content. Motivated by the increasing costs and environmental impacts of virgin aggregate extraction, this study aims to develop an alternative road base design using locally available waste materials. This study investigates the beneficial reuse of waste materials by improving RCA with other waste-based materials. The enhanced RCA was designed as the fine fraction (2 mm–0.075 mm), whereas basalt aggregate (BA) was used as the coarse skeleton (19 mm–0.475 mm). Selecting RCA below 2 mm was intended to mitigate the adverse effects of its porous adhered mortar and to promote stronger bonding with pozzolanic wastes. The experimental program comprised (i) compaction tests, (ii) soaked CBR tests on BA with RCA replacement levels up to 45%, and (iii) UCS tests to identify the optimal stabilizer blend by varying CCS:SSA ratios (2:8 to 4:6), RCA contents (20% to 40%), and curing period (0–28 days). Based on the UCS outcomes, CBR tests were repeated at 7 and 14 days using a fixed RCA–BA ratio while adding CCS and SSA at 10–30% to quantify the improvement efficiency. Finally, the mixture yielding the highest soaked CBR was validated by a cyclic plate load test as a small-scale performance check.

Coarse aggregates form the structural framework of base layers and govern resistance to repeated traffic and environmental loads, including permanent deformation [52–55]. Accordingly, untreated BA was selected as the coarse fraction, while the waste-derived fine fractions (RCA, SSA, and CCS) were used to fill voids and progressively enhance inter-particle bonding. As reported in the literature, such fine fractions can reduce permeability, limit pore water pressure buildup, mitigate thermal cracking risk, and improve durability against environmental actions [29,56]. Moreover, CCS and SSA are expected to compensate for typical RCA drawbacks such as low strength, high porosity, and high water absorption [13,16]. The experimental study designed for this purpose is detailed in the methodology section. The flow chart for this study is presented in Figure 1.

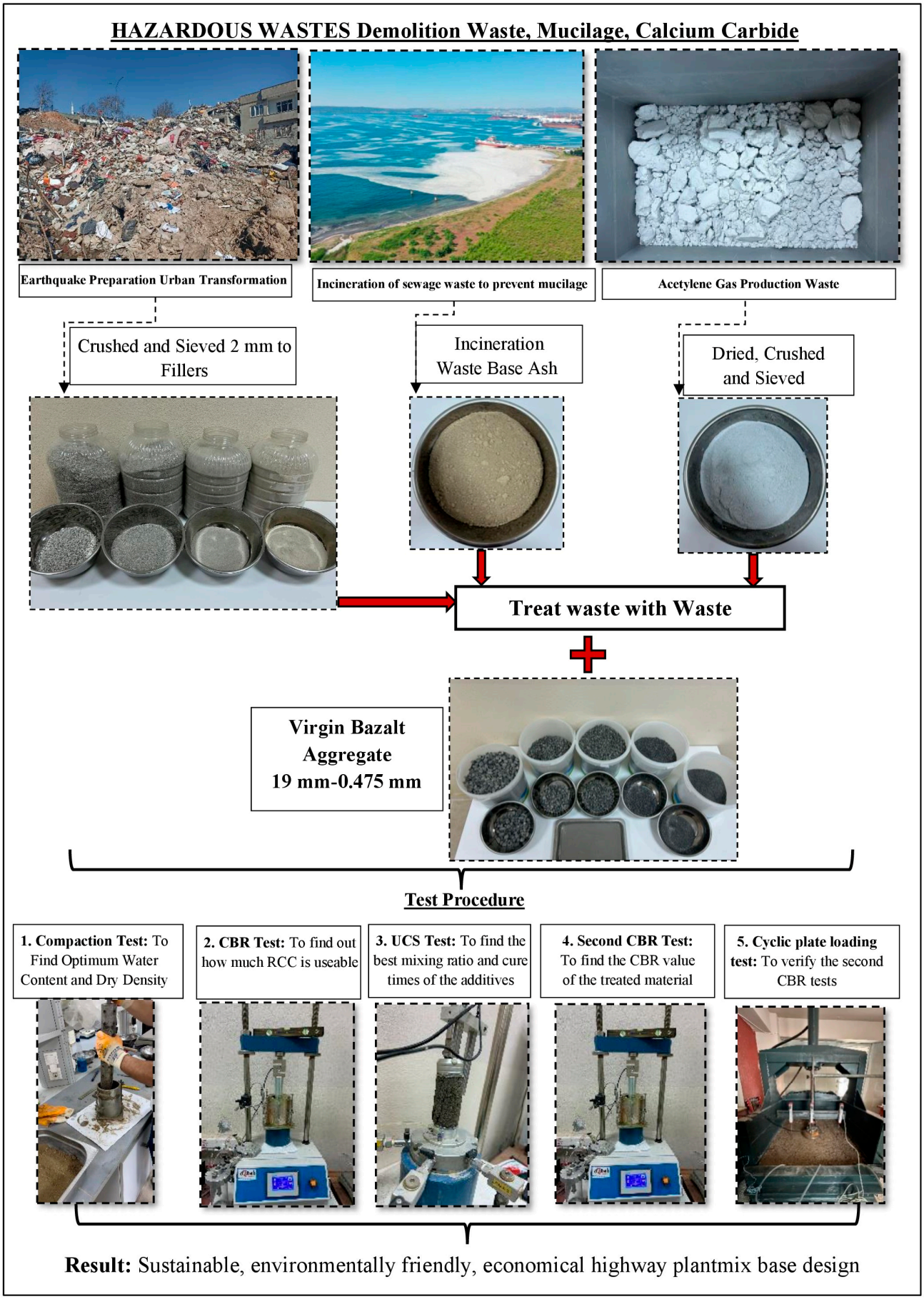


Figure 1. Flow chart of the study.

2. Materials and Methods

A total of four different materials were used in this study. The materials utilized include basalt aggregate (BA), sourced from a quarry; recycled concrete aggregate (RCA), obtained from demolished buildings due to urban renewal; sewage sludge ash (SSA); and carbide sieve sludge (CCS). Detailed information about these materials is as follows.

2.1. Basalt Aggregate (BA) Sourced from the Quarry

The natural, virgin basalt aggregate used in this study was supplied from the basalt quarry operated by Efor Mining Company, located within Irşadiye neighborhood, Gölcük district, Kocaeli province, Türkiye. Various properties of the basalt aggregate are provided in Table 1 below. The largest particles can pass through a 22 mm sieve, while the smallest particles are of filler size (0.075 mm). The material, initially obtained in a mixed gradation, was sieved before use (Figure 2).

Table 1. Efor Mining Company basalt quarry aggregate properties [57].

Test	Related Specification Number	Result (%)	Specification Limits
Mg_2SO_4 Freezing Loss (%)	TS EN 1367-2	1.5	Max. 14%
L.A. Abrasion loss (%)	TS EN 1097-2	15	Max. 25%
Flatness Index (%)	BS 812	12	Max. 25%
Plasticity Index, (%)	TS-1900	NP	NP
Water Absorption (%)	TS EN 1097-6	Course: 0.64; Fine: 0.66	Max. 2%
Peeling Resistance (%)	KTŞ Kısım 403 Ek-A	70–75	Max. 60%
Methylene Blue Test, (Stone Dust) (%)	TS EN 933-9	0.8	Max. 1.5%
Specific Gravity:		Course: 2.663 Fine: 2.701 Filler: 2.716	

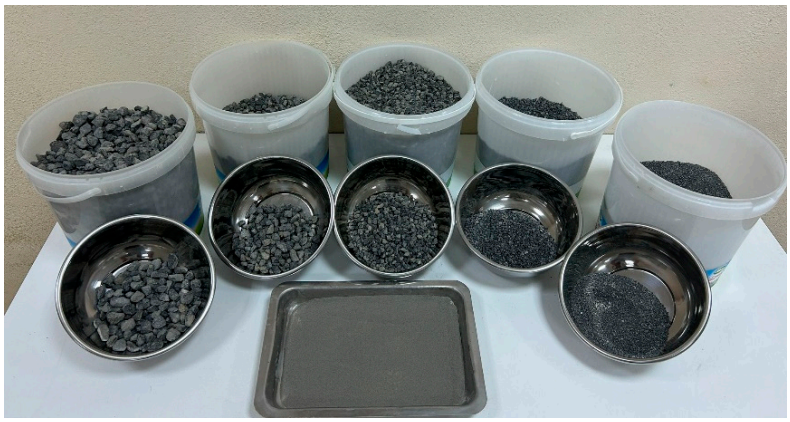


Figure 2. Sieved and laboratory-stored basalt aggregate (19 mm–0.475 mm).

2.2. Recycled Concrete Aggregate (RCA)

The recycled concrete aggregate (RCA) used in this study was obtained from a demolished building during urban renewal projects in Yalova, a city located on the North Anatolian Fault Line, where 2504 people lost their lives in the 1999 Gölcük earthquake. The demolished structure was a residential building located at parcel 271, block 2, in the Dörtyol area of Gazi Osman Paşa Neighborhood. Before demolition, core samples were taken from the building, and the average compressive strength was recorded as 11.4 MPa. The concrete debris brought to the laboratory was processed using a Dotek (Ankara/Türkiye) brand

2015 model Los Angeles abrasion machine to break it down for experimental use. Similar studies in the literature have utilized this method [27,58,59]. This method has also been applied to remove cement mortar from the aggregate [59,60]. As seen in Figure 3, the RCA was classified into different sieve sizes in the laboratory. As previously stated, coarse aggregates were obtained from BA, while fine aggregates were sourced from waste materials. As can be seen in Figure 4, there were coarse aggregates where the aggregate and cement paste attached after the RCA was crushed. In these aggregates, the interface between the cement paste and the aggregate forms a weak zone, which is a common issue with RCA. This weak zone arises due to micro-cracks and voids present in the cement paste [59]. From a microstructural perspective, SEM-based studies report that RCA particles are natural aggregates partially coated with a porous and microcracked layer of old cement mortar. This residual mortar increases the total pore volume and explains the significantly higher water absorption of RCA compared to untreated aggregates. This is consistent with the higher OMC observed in RCA-rich mixtures in the present study [61]. Therefore, it was considered more suitable to use RCA as fine aggregate rather than coarse aggregate. Figure 5 presents hand microscope images of fine RCAs, showing that the cement paste–aggregate bond is stronger in fine RCA. This is because the micro-roughness of the cement paste allows better adhesion at smaller scales. This property prevents sudden fractures in coarse RCA, which could otherwise lead to new void formations and structural weaknesses.



Figure 3. (**A**) Area where concrete debris is collected. (**B**) Crushed and sieved concrete aggregate.

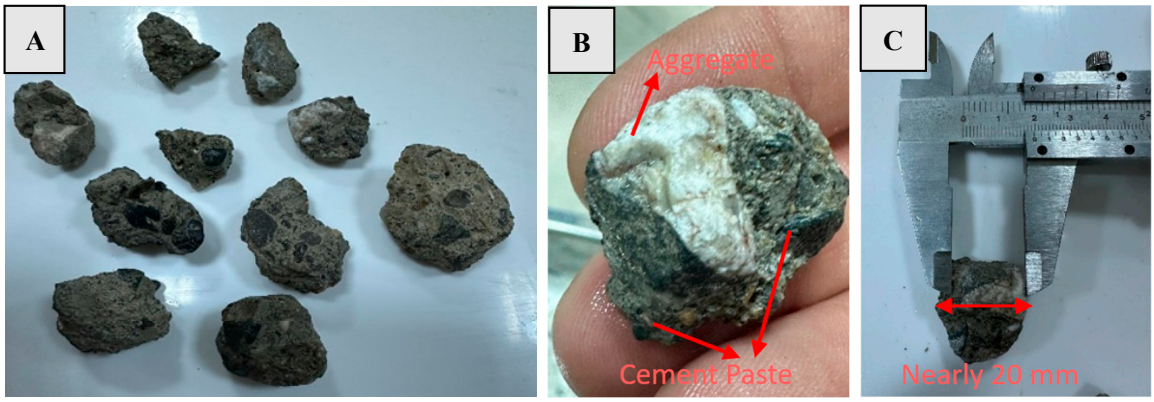


Figure 4. (**A**) RCA; (**B**) cement paste and aggregate interfaces; (**C**) coarse aggregate size.

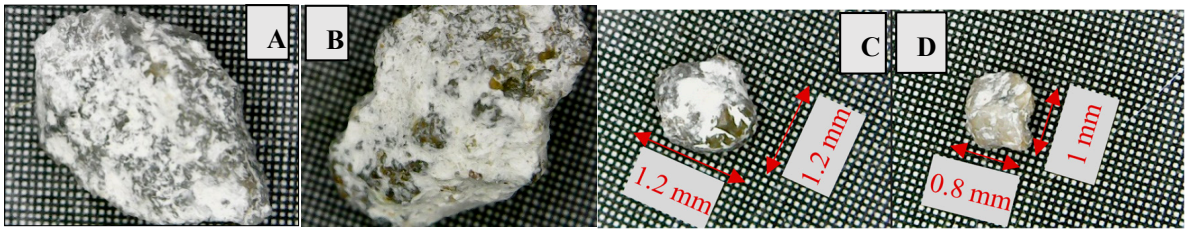


Figure 5. (**A**,**B**) Images of fine RCA observed under a light microscope. (**C**,**D**) Fine aggregates' size at grid spacing 0.1 × 0.1 mm.

2.3. Sewage Sludge Ash (Bottom Ash) (SSA)

Due to the mucilage problem in the Marmara Sea, studies have been conducted to reduce sewage waste in coastal provinces. One of the most used methods in these efforts is solid waste incineration plants. Within this scope, SSA used in this study was obtained from the sewage sludge incineration and energy recovery facility operated by Bursa Metropolitan Municipality. In the literature, SSA is described as a material rich in aluminum silicate [12,13]. Bottom ash accounts for 80–90% of the total waste mass [62]. In this study, bottom ash (SSA), which is produced in large quantities by mass, was utilized. The physical properties and composition of SSA, obtained through X-ray fluorescence spectrometry (XRF) (excluding compounds present in amounts less than 1%), are provided in Tables 2 and 3, based on data from the supplying facility. SSA can cause heavy metal leakage when used in high quantities, but previous studies have indicated that this leakage is greatly reduced in an alkaline environment, when bonds are formed, and when low particle sizes are used. In this study, SSA will not exceed 7.35% by mass even at the highest rate. Furthermore, the CCS used is an alkaline source and will form C-S-H bonds with SSA. Finally, since the SSA particle size will be 75 microns or less, it is expected to form bonds actively [63–66]. When SEM images of SSA are examined in the literature, they predominantly show irregular grains and strongly developed, porous surfaces, consisting of angular particles. This type of rough and porous texture can trap water and increase water demand. When mixed with SSA binders, it provides potential nucleation sites for the precipitation of reaction products. However, during this process, the bonds formed with CCS can convert the weak areas that hold water into C-S-H bonds over time [65,67].

Table 2. Physical properties of SSA.

Physical Properties	
Sieve Size %	Passed from 0.075 mm sieve %95.6
Specific Gravity	2.32
pH Value	12.2
Density (ton/m^3)	0.477

Table 3. The compounds and their proportions in SSA were determined by XRF analysis.

X-Ray Fluorescence Spectrometry (XRF) Results:							
SiO_2	Al_2O_3	Fe_2O_3	CaO	P_2O_5	MgO	Na_2O	loss of ignition
31.651%	7.965%	9.718%	22.973%	10.21%	3.497%	2.213%	3.53%

The chemical composition of municipal solid waste bottom ash includes 22.97% CaO and a total of 49.33% of SiO_2-Al_2O_3-Fe_2O_3 components. When the proportions are examined, it is observed that the CaO content meets the standard, while the total of the other components does not fully meet the 50% requirement, but is close to the threshold. Additionally, the SO_3 and loss on ignition (LOI) values were found to be low, as required by

the standard [68]. In the literature, it has been stated that waste sludge bottom ash contains larger particles compared to fly ash, which leads to lower compressive strength [13]. In this study, to eliminate the disadvantage of large particles, material sieved through a 0.075 mm sieve was obtained from the municipality (Figure 6).



Figure 6. SSA and CCS used in the studies.

2.4. Calcium Caride Sludge (CCS)

The carbide sludge used in this study was obtained from the Linde Gas Inc. facility, which operates in the Başkent Organized Industrial Zone located in Sincan, Ankara, Türkiye. The fully water-saturated carbide sludge was first dried at 105 °C for 24 h in the Yalova University Laboratory, then ground and sieved through a 0.075 mm sieve before use (Figure 6). The XRF analysis results of the carbide sludge are presented in Table 4. Compounds with a content of less than 1% are not included in the Table 4. Upon examining Table 4, it is observed that the CaO content is quite high (88.19%). However, the literature indicates that the calcium-containing compound with binding properties is $Ca(OH)_2$. During the XRF test, at 550 °C, H_2O is released from the $Ca(OH)_2$ composition as a gas, leaving behind CaO, which is why CaO appears in the results [28].

Table 4. The compounds and their proportions in CCS were determined by XRF analysis.

X-Ray Fluorescence Spectrometry (XRF) Results:							
CaO	SiO_2	Al_2O_3	Fe_2O_3	SO_3	MgO	SrO	loss of ignition
88.19%	2.583%	1.611%	0.4147%	0.8416%	3.356%	0.028%	2.85%

In this study, the use of a mixture of waste materials, RCA, CCS and SSA, along with BA as a plantmix base material in highways was investigated. To ensure resistance to repeated traffic loads, natural aggregate was used as coarse aggregate (19 mm–0.475 mm), while the mixture of RCA, CCS, and SSA was designed to serve as fine aggregate (below 2 mm–0.075 mm). This fine aggregate mixture was intended to fill the voids between coarse aggregates, provide structural support, and enhance strength over time by forming calcium silicate hydrate (C-S-H) bonds. Additionally, it was designed to reduce permeability, prevent the development of excessive pore water pressure, delay thermal cracking, and improve durability. Due to the necessity of mixing four different materials in specific ratios, the plantmix base design was chosen, as it was considered to facilitate easier field application. The study was conducted following the standards outlined in the Highway Technical Specifications (KTŞ) issued by the General Directorate of Highways of the Republic of Türkiye [57]. In Figure 7, the granulometric curve presents the limits, tolerances, and mixture gradation lines for the plantmix base. The black line in the curve represents the gradation prepared for CBR tests and repeated plate loading tests. According to the Highway Technical Specifications (KTŞ), in the largest diameter part of the curve, it is

desired to use aggregates passing through a 25 mm sieve for the plantmix foundation. However, since the use of 25 mm particles is not recommended in CBR tests, the 25 mm sieve was excluded from the granulometric curve for the entire study [69].

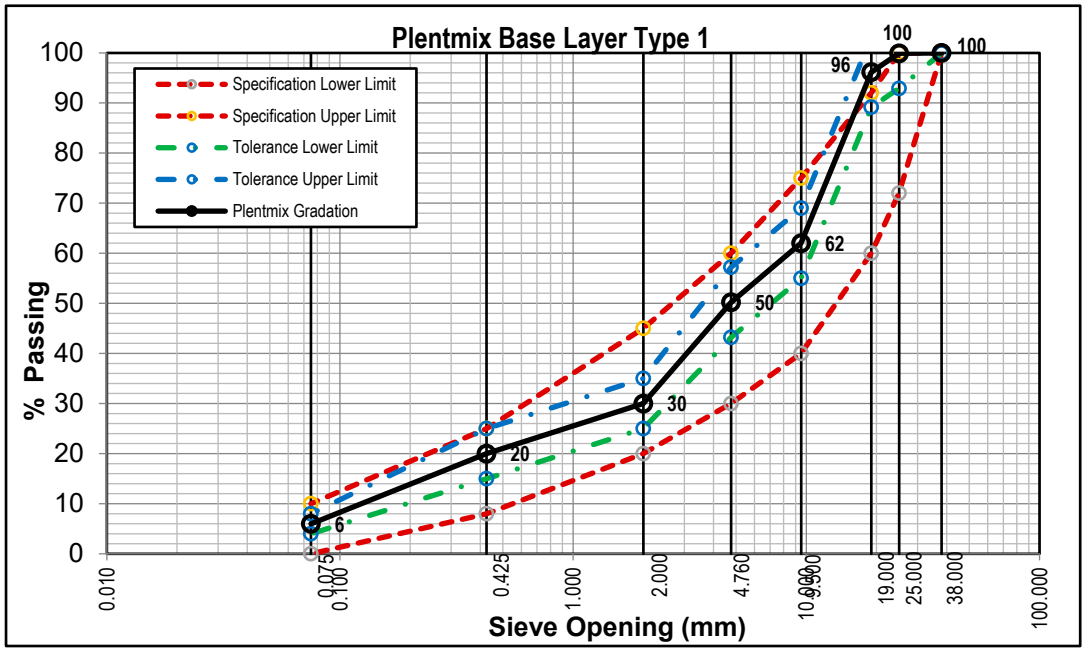


Figure 7. Granulometric curve of the plantmix foundation used in CBR tests.

The experimental study consists of several stages. Accordingly, compaction tests were first carried out, and optimum moisture content and dry unit weight data required for different tests were obtained. In the second stage, CBR tests were carried out. At this stage, RCA was mixed with BA in specific ratios without any additives. This allowed for the determination of the RCA content level at which the CBR limit set by KTŞ would be exceeded. Subsequently, unconfined compression tests were conducted to examine the optimal SSA and CCS mixture ratios and curing periods that provide the highest compressive strength. In the next step, a second round of CBR tests was performed, in which SSA and CCS were added to RCA as stabilizing materials. In the final stage, the optimal mixture determined from previous tests was subjected to a cyclic plate loading test [70].

2.5. Compaction Tests for Experiments

In the experimental study, Proctor tests were conducted according to ASTM standards to determine the optimum moisture content and dry unit weight of the mixtures [71,72]. According to Table 8.13 in the Soil and Stabilization Laboratory Handbook published by the General Directorate of Highways in 2021, when looking at the aggregate diameters and ratios, it has been determined that CBR and cyclic plate loading tests should be performed with a modified Proctor, and unconfined compression tests should be performed with a standard Proctor. The samples were impacted with 2700 kJ/m^3 of energy using the modified Proctor method and with 600 kJ/m^3 of energy using the standard Proctor test [69,73]. For Proctor tests, the increase in water content in the mixture to be used in CBR tests rapidly decreases the CBR values [74]. Therefore, in this study the optimum water content was determined with precision.

2.6. Stage 2: CBR Tests Applied Only to the BA and RCA Mixture

In this part of the study, RCA was added to BA in different ratios, and the soaked CBR values were compared. Accordingly, the samples with RCA added at ratios of 0, 25, 35 and 45% compared to the total mass and without any additional additives, the details of which are given in Table 5, were subjected to the CBR test after being kept in a water pool for 4 days (96 h) with at least 2.5 cm of water covering them without any curing. Percentage by weight of the mixture was adjusted according to the sieve ranges and ratios given in Table 5. In the CBR test, the sample was compressed in three layers, with 56 blows in each layer.

Table 5. Percentage by weight of the mixture obtained by adding RCA at different ratios.

Aggregate Source	Basalt Aggregate (BA) (%)						RCA (%)			
Sieve Ranges	19–9.5	9.5–4.76	4.76–2	2–0.475	0.475–0.075	Filler	4.76–2	2–0.475	0.75–0.075	Filler
100% BA	29.348	16.304	16.304	16.304	15.217	6.523				
75% BA + 25% RCA	29.348	16.304	16.304	13.043	0	0	0	3.262	15.217	6.522
65% BA + 35% RCA	29.348	16.304	16.304	3.043	0	0	0	13.262	15.217	6.522
55% BA + 45% RCA	29.348	16.304	9.348	0	0	0	6.957	16.304	15.217	6.522

As shown in Table 5, when more than 45% RCA was added, RCA would replace BA, which was originally designed as coarse aggregate. Therefore, higher RCA ratios were not tested. During the CBR tests, the results were obtained after applying the corrections specified in the Soil and Stabilization Laboratory Manual, published by the General Directorate of Highways in 2021. Accordingly, standard weights were placed on top of the samples to represent pavement layer, both while they were in the water pool and while they were being tested. Accordingly, three standard 2.27 kg weights were used to represent the 20 cm pavement thickness. Swelling readings were made on the samples but were not specified separately since they were very small. When the resulting stress/penetration graph was convex instead of concave, correction was made, and the experiment was repeated when the result changed more than 1.25 mm horizontally. If the CBR result at a penetration depth of 5.08 mm deviated by more than 10% from the CBR result at a penetration depth of 2.54 mm, the test was repeated. In other cases, the higher CBR value was used. Finally, at least two tests were conducted for each mixture type, and the average of the results was taken. If the difference between the two test results exceeded 20%, a third test was performed, and the average of the two closest CBR values was used [69].

2.7. Determination of the Optimal SSA/CCS Ratio and Curing Duration Using the Unconfined Compression Test

Due to the large amount of material and labor required in CBR tests, it was decided to use the unconfined compression test to determine the optimal binder ratio and curing duration. Although there is no direct correlation between CBR and unconfined compression strength in the literature, previous studies indicate that unconfined compression test results can be used as a guideline [75,76]. On the other hand, since SSA and CCS will close the voids with the bonds they form together, thus resulting in higher UCSS test results, unlimited pressure tests were used to determine the ideal SSA/CCS ratio and curing time that will form a strong bond between RCA, SSA, and CCS used as fine aggregate to determine the best bonding ratio. The use of unconfined compression tests to determine weight mixture ratios is a widely accepted method in the literature (Table 6) [56].

Table 6. Percentage by weight of the mixture for the unconfined compression test.

Ratio of Basalt Aggregate, RCA and Additive (CCS/SSA)	Basalt Aggregate (BA) (%)				RCA (%)			Additive (%)	
	4.76–2	2–0.475	0.475–0.075	Filler	2–0.475	0.475–0.075	Filler	CCS	SSA
%65 BA %35 RCA	16.25	16.25	16.25	16.25	11.66	11.66	11.68	0	0
%65 BA %35 RCA %10 ADD. 2/8	16.25	16.25	16.25	16.25	11.66	8.16	11.68	0.7	2.8
%65 BA %35 RCA %10 ADD 3/7	16.25	16.25	16.25	16.25	11.66	8.16	11.68	1.05	2.45
%65 BA %35 RCA %10 ADD 4/6	16.25	16.25	16.25	16.25	11.66	8.16	11.68	1.4	2.1
%65 BA %35 RCA %20 ADD 2/8	16.25	16.25	16.25	16.25	8.16	8.16	11.68	1.4	5.6
%65 BA %35 RCA %20 ADD 3/7	16.25	16.25	16.25	16.25	8.16	8.16	11.68	2.1	4.9
%65 BA %35 RCA %20 ADD 4/6	16.25	16.25	16.25	16.25	8.16	8.16	11.68	2.8	4.2
%65 BA %35 RCA %30 ADD 2/8	16.25	16.25	16.25	16.25	6.42	6.42	11.66	2.1	8.4
%65 BA %35 RCA %30 ADD 3/7	16.25	16.25	16.25	16.25	6.42	6.42	11.66	3.15	7.35
%65 BA %35 RCA %30 ADD 4/6	16.25	16.25	16.25	16.25	6.42	6.42	11.66	4.2	6.3
Cont.Exper. %20 ADD %100 SSA	16.25	16.25	16.25	16.25	8.16	8.16	11.68	0	7.00

In the unconfined compression tests, based on the results obtained in Step 2, RCA was added to the BA at a constant mass ratio of 35%. The SSA and CCS additives were adjusted to 10%, 20%, and 30% of the RCA mass. The reason for not exceeding these levels is that SSA and CCS act as fillers, and according to the Highway Technical Specifications (KTŞ) as seen in the granulometric curve in Figure 7, the maximum allowable filler content is around 10–12%. Since CCS and SSA mixtures require long curing times [25,29], the tests were repeated at different curing durations: 0, 7, 14, and 28 days. The CCS/SSA ratio in the mixture was set at 2/8, 3/7, and 4/6.

In the literature, similar studies using various ashes from different sources mixed with carbide sludge have reported high compressive strength results at approximately these proportions, where the ash content is higher and the carbide sludge content is lower [5,11,16,17,56,77]. The variation in the optimal mixture ratios observed in different studies is primarily due to differences in the materials used, their composition, and their physical properties, as well as the presence of other materials in the mixture [29]. Additionally, materials formed through combustion processes, such as fly ash, can exhibit changes in composition even when sourced from the same provider at different times [78].

The samples prepared for the unconfined compression test had a diameter of 50 mm and a height of 100 mm and were formed using a split mold. The compaction energy applied was consistent with the standard Proctor test, based on volume ratio calculations (three layers with a total of 19 blows). As indicated in the literature, the unconfined compression tests were conducted using materials passing through a 4.76 mm sieve opening [56,69]. Based on this requirement, the mixture ratios were readjusted accordingly. The materials were dry-mixed for five minutes, followed by an additional five minutes of mixing with water. For each different mixture type, three specimens were prepared and tested, and the average value was used for analysis. During the curing period, the specimens were stored at 21 °C with over 95% relative humidity. Additionally, the samples were wrapped with two layers of stretch film to maintain moisture levels. A loading rate of 1 mm/min was applied during the tests (Figure 8).

2.8. CBR Tests of Waste-Enhanced RCA and BA Mixture

In this part of the study, SSA and CCS mixtures were used as filler material in the samples subjected to CBR tests. The procedure applied in the CBR method of Stage 2 was repeated in this stage, with the difference that before the soaking process, the CBR samples were cured in a desiccator at a temperature of 21 °C and a humidity of at least 95%. Curing before soaking is a method applied in the literature [5]. At this stage, the effect of SSA and CCS additives in the mixtures was examined. Therefore, 35% RCA was added by total mass

to the mixture. Instead of the filler part of this RCA material, binder was added at ratios of 10, 20 and 30% by mass of RCA. The ratio of the binder materials was kept constant, and the CCS/SSA ratio was determined as 3/7 (based on the highest unconfined compressive strength value obtained in Stage 2). The samples were cured for 7 and 14 days, then soaked in water for 4 days before testing.



Figure 8. Unconfined compression test study: (**A**) Prepared mixture materials. (**B**) Sample preparation mold. (**C**) Curing cabinet and prepared samples.

2.9. Cyclic Plate Loading Tests

In the final part of the study, a cyclic plate loading test was conducted to verify the obtained CBR values. In highway foundations, high resilient modulus (high strength) values enable cost-effective pavement designs by allowing for more economical structural designs [79]. This test is usually performed in accordance with internationally recognized standards such as ASTM D1195/D1195M-21 and DIN 18134 [80,81]. However, these standards are designed for field applications, and the data obtained from these tests are generally used to estimate California Bearing Ratio (CBR) values using established empirical correlations. To ensure the validity of these estimates, laboratory-scale experiments are also conducted using specially designed apparatus that simulates field loading conditions. A significant number of studies have addressed this approach and examined its reliability [82–90]. The mixture details for the plate loading test are provided in Table 7. In this mixture, 35% of the total weight consists of RCA, and 30% of RCA by weight consists of CCS/SSA mixture. CCS/SSA ratio was taken as 3/7. Approximately 400 kg of material was used in the plate loading test. The material was placed in four layers of 100 kg each. After each layer was placed, a compaction process was performed, ensuring that at least 95% of the modified Proctor density was achieved. Beneath the designed plantmix base, there was a 25 cm thick subbase layer. After 14 days of curing, the cyclic loading test was carried out. The material for the tests was prepared in the steps shown in Figure 9 below; the materials were mixed for 10 min using a panmixer. Three straingauge (SG) plantmixes were placed at half the height of the foundation. The SG in the middle was horizontal, and the ones on the sides were placed vertically and horizontally. There was a load cell (LC) on the loading piston. A pressure cell (PC) was placed just above the subbase, under the load. For measuring vertical displacements, three potentiometric rulers (LVDT) were placed as shown in the figure (Figure 10). One of the rulers was planned to determine the sinking amount on the loading plate and the other two were planned to measure the swelling amounts. Loading was performed with 35 kN cyclic loads. This load is approximately half the axle equivalent of a loaded truck load measured in the field [91]. A circular plate with a diameter of 30 cm was used as the loading plate. The experiment was stopped when the displacement difference had similar values in 50 cycles. A summary of the experiments is given in Table 8.

Table 7. Percentage-by-weight mix ratios used in cyclic plate loading test.

CONTENTS	w opt. Su %	Basalt Aggregate				Urban Transformation			Binder	
BA: Basalt RCA: Recycled Concrete Aggregate CCS: Carbide Mud SSA: Waste Mud Ash		19–9.5	9.5–4.76	4.76–2	2–0.475	4.76–2	2–0.475	0.475–0.075	CCS	SSA
%35RCA %30 Add. (3/7 CCS/SSA) (%)	9.37	29.35	16.30	16.30	3.04	0	13.26	11.24	3.15	7.35



Figure 9. (**A**) Subbase; (**B**) RCA, SSA, and CCS used in each layer; (**C**) mixing processes.

Table 8. Summary of test program.

Reusing RCA by Enhancing It with Other Waste Materials (Treating Waste with Waste)		
Experiment	**Purpose and Conditions**	**Variables**
Compaction Test	Finding Optimum Water Content and Dry Unit Weight of RCA and BA mixture. (These ratios were used in subsequent experiments.)	The Ratio of Basalt Aggregate and Recycled Concrete Aggregates: %100 BA, %75BA–%25RCA, %65BA–%35RCA, %55BA–%45RCA
Soaked CBR	Determining the maximum RCA ratio (without additives) permitted in the specifications. (To be improved with waste materials in subsequent experiments.)	The Ratio of Basalt Aggregate and Recycled Concrete Aggregates: %100 BA, %75BA–%25RCA, %65BA–%35RCA, %55BA–%45RCA
UCS	Determining the ratio and participation amounts of waste materials that produce the best results when mixed together, with C-S-H bonds filling the gaps.	There are three variables: curing time (0, 7, 14, 28 days), additive ratio (%10, 20, 30) and additive content (CCS/SSA: 2/8, 3/7, 4/6).
Soaked CBR	Determining the CBR results of different additive ratios (additives were used instead of filler material in the RCA).	Cure Time and Additive Ratio (%10, 20 and 30)
Cyclic Plate Loading Test	It has been used as a different experimental method to verify CBR results.	%65 BA %35 Waste Materials (%24.5 RCA %10.5 Additive (3/7 CCS/SSA))

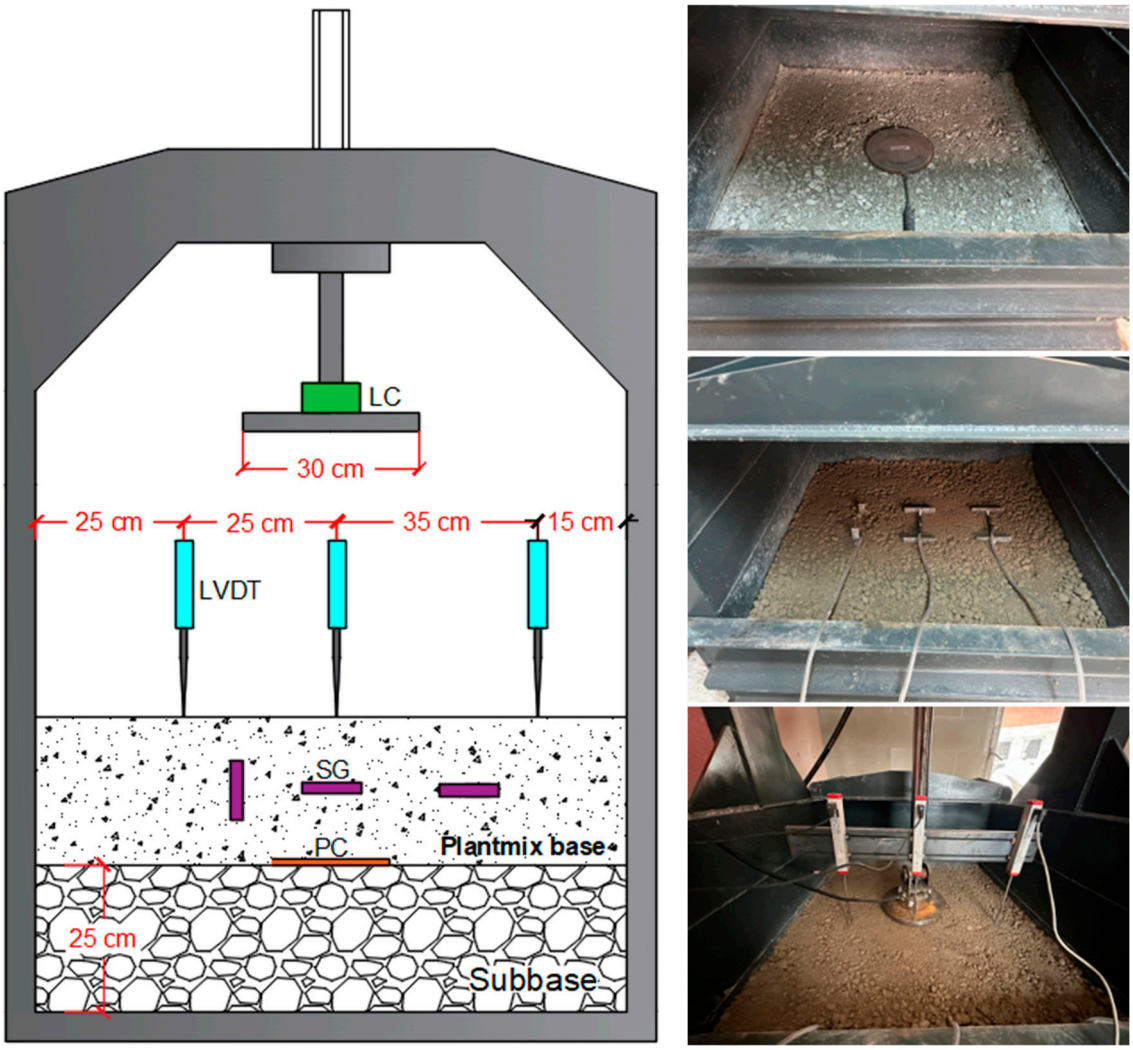


Figure 10. Setup for cyclic plate loading test.

3. Results and Discussion

In this study, a common solution developed to address two major disaster risks—earthquakes and environmental pollution—was examined. The findings were presented within the context of Yalova as a case study. Due to the presence of fertile plains, greenhouse farming and floriculture are widely practiced in Yalova. In the event of the demolition of approximately 6000 housing units classified as high-risk, the use of agricultural land for debris storage would become inevitable. Another environmental pollution issue affecting Yalova, a province on the shores of the Marmara Sea, is marine mucilage, which negatively impacts marine life and emits an unpleasant odor. Sewage discharge plays a significant role in mucilage formation, making solid waste incineration facilities a recommended solution. These facilities generate ash waste (both bottom and fly ash) as a byproduct. Additionally, Yalova is home to several shipyards where acetylene gas is used for welding purposes. The production of this gas results in the formation of calcium carbide sludge, which is another source of environmental pollution. This study proposes a design that utilizes these three waste materials together to create a beneficial solution. The findings indicate that, due to its structural properties, RCA can effectively serve as fine aggregate in the mixture. Furthermore, the addition of pozzolanic SSA and binding CCS enhances its characteristics. As a result, the study confirms that demolition waste from buildings can be repurposed as a highway plantmix base. The key findings of the study are as follows.

3.1. Compaction Test Results

Compaction tests were first applied to BA and RCA mixtures. Modified Proctor results without other additives are given in Table 9.

Table 9. Results of modified Proctor tests on BA and RCA mixtures.

Mixture	w (%)	γ_{dry} (kN/m^3)
100% BA	7.12	21.17
75% BA 25% RCA	8.09	20.47
65% BA 35% RCA	8.76	20.375
55% BA 45% RCA	9.06	19.82

The results indicate that virgin basalt aggregate has the highest dry unit weight and the lowest optimum moisture content. This is expected due to the dense, non-porous structure of basalt aggregate, which limits its water absorption capacity. In the literature, results of modified Proctor tests conducted on basalt samples from six different regions indicate that the optimum moisture content varies between 6% and 9%, while the dry unit weight ranges from 21.8 to 23.1 kN/m^3 [92]. The values obtained in this study are consistent with the reported literature data. Furthermore, an analysis of the mixture results reveals that as the RCA content increases, the optimum moisture content also increases, while the dry unit weight decreases. This can be attributed to the porous nature of RCA, which leads to higher water absorption and a reduction in dry unit weight. Similar findings have been reported in the literature for recycled concrete aggregate mixtures [1,12,13,93]. Both SSA and CCS added to the mixture had low density and high water retention capacity. As a result, they increased the optimum moisture content while reducing the dry unit weight. In the mixtures used for the UCS test, the dry unit weight ranged from 12.84 to 13.28 kN/m^3, while the optimum moisture content ranged from 14.01% to 14.83% (Table 10). These results are as expected and are due to the porous structure of SSA and the water-retaining properties of CCS. The lower density of both additives compared to both BA and RCA also contributed to the reduction in dry unit weight.

Table 10. Results of standard Proctor tests on additive and RCA mixtures.

Mixture	w (%)	γ_{dry} (kN/m^3)
20% Additive (2/8 CCS/SSA)	14.01	13.28
30% Additive (2/8 CCS/SSA)	14.83	12.84
20% Additive (100% SSA)	14.23	13.44

3.2. CBR Results of BA and RCA Mixtures

The samples prepared by mixing basalt aggregate with RCA at ratios of 0, 25, 35 and 45% were subjected to soaked CBR tests and the results shown in Figure 11 were obtained.

When the results are examined, it is seen that the sample consisting of 100% basalt aggregate has a CBR of 187%, and this value is in accordance with the literature information [92]. When 25% RCA was added, the CBR value decreased to 182%, and the sample consisting of 100% BA was close to the CBR result. When the RCA content was 35%, the CBR value was 113%, which did not fully meet the 120% CBR requirement specified for plantmix bases in KTŞ but was close to the target value. This suggests that further enhancement efforts could potentially increase the CBR value beyond 120%. On the other hand, when the RCA content increased to 45%, the average CBR value dropped significantly to 57%. This 57% value represents the average of three different test results conducted on the mixture. Some inconsistent results were observed in the CBR tests. Among the three tests

conducted, CBR values of 18%, 65%, and 49% were recorded. The 18% value was excluded from the average calculation due to its significant deviation. The reason for the difference in value occurring over 3.5 times is that too much RCA was used and, as can be seen in Table 5, coarser material passing through a sieve with a 4.76 mm opening was used so that the gradation curve given in Figure 7 did not change. The replacement of BA with coarser RCA particles resulted in irregular fractures between the cement paste and aggregate, leading to localized weaknesses in areas where these fractures aligned with the CBR piston, ultimately reducing the measured CBR values. Recycled concrete aggregate (RCA) has low strength values, high water absorption capacity, and high porosity, so its properties are improved with cement, lime, or fly ash [13,16,18]. Due to these findings, it was concluded that using 45% RCA could not be improved even with further modifications. As a result, mixtures containing 45% RCA were excluded from subsequent stages of the experiments.



Figure 11. CBR test results applied to RCA and BA mixtures.

3.3. Unconfined Compression Test Results

The results of the unconfined compression test conducted to find the appropriate ratio between SSA/CCS mixtures and to examine the effect of the curing time are given in Table 11 and Figure 12 below.

Table 11. Unconfined compression test results (kPa).

Mixture Ratios	0 Day	7 Day	14 Day	28 Day
65BA% 35RCA% 0% admixture (kPa)	26.80			
10% admixture CCS/SSA: 2/8 (kPa)	78.60	81.35	72.65	98.27
10% admixture CCS/SSA: 3/7 (kPa)	84.15	78.80	83.38	138.78
10% admixture CCS/SSA: 4/6 (kPa)	107.16	114.22	127.24	143.39
20% admixture CCS/SSA: 2/8 (kPa)	125.08	180.18	198.79	245.52
20% admixture CCS/SSA: 3/7 (kPa)	113.17	245.37	397.06	405.02
20% admixture CCS/SSA: 4/6 (kPa)	144.79	327.59	484.23	556.90
30% admixture CCS/SSA: 2/8 (kPa)	107.15	345.46	603.36	705.21
30% admixture CCS/SSA: 3/7 (kPa)	123.10	243.01	640.29	771.32
30% admixture CCS/SSA: 4/6 (kPa)	102.31	262.07	625.40	666.49
Cont.Exper. %20 ADD %100 SSA	75.25	84.43	88.45	90.69

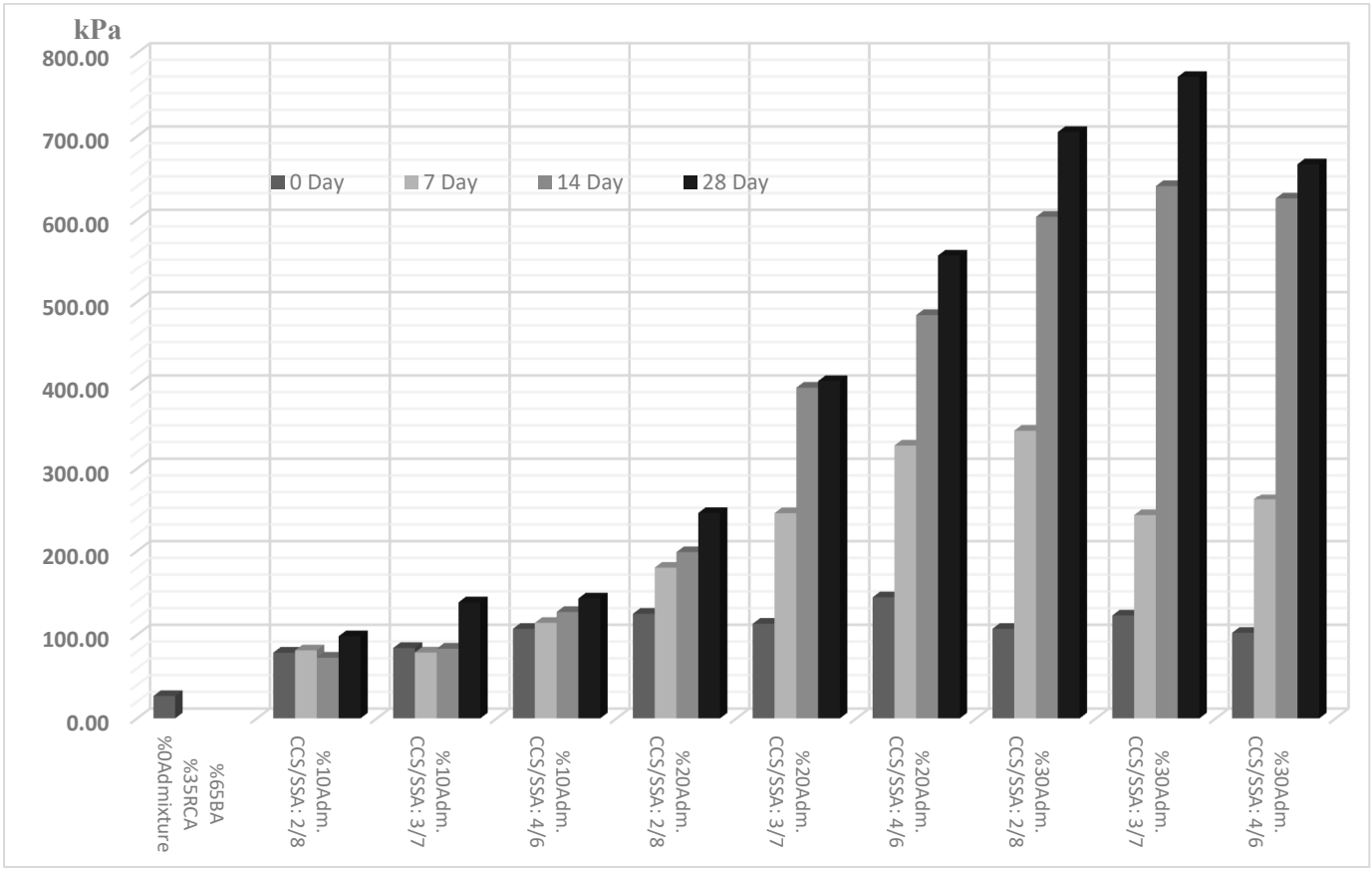


Figure 12. Unconfined compressive strength (UCS) results.

The analysis of the UCS test results reveals that the sample without any additives exhibited a compressive strength of 26.80 kPa. However, samples containing SSA and CCS demonstrated at least 2.71 times higher compressive strength, confirming the positive impact of these additives. This improvement became more pronounced as the binder content and curing duration increased. The highest UCS value was recorded in 28 days of curing at 30% binder ratio and reached a value 28.7 times (771.32 kPa) higher than the sample with no binder added. When examining the CCS/SSA ratio, the most significant strength improvements were observed at 3:7 during both 14-day and 28-day curing periods. Based on these findings, the optimal combination for achieving high strength values in UCS tests involves 30% binder content, CCS/SSA ratio of 3:7, and minimum curing period of 14 days. These results align with findings in the literature, which indicate that calcium-based binders and fly ash-containing materials require at least 14 days of curing to form sufficient bonding [13,17,25,27,29]. The results confirm each other with the microstructural results in the literature. In microstructure investigations reported in the literature, it has been noted that when a high amount of CCS is used, unreacted $Ca(OH)_2$ crystals are frequently observed; these crystals are in the form of hexagonal plates and cause the structure to become more porous and voided [94,95]. On the other hand, when CCS is used together with silica-rich materials (such as fly ash or sewage bottom ash), it undergoes pozzolanic reactions and forms C–S–H bonds. The two materials complement each other by filling the voids and creating a higher-strength structure. This has also been confirmed in XRD and SEM results, where a denser structure with reduced voids was observed [36]. In another microstructure study from the literature, SSA and CCS were used together, and gypsum was also added to enhance the reaction. The results showed that more hydration products were formed in microstructural analyses, and a geopolymer with a

high compressive strength of about 53 MPa was obtained. In this case, ettringites formed due to the presence of gypsum, and these ettringites contributed to filling micro-voids; however, it was emphasized that to achieve such values, the CCS and activator ratios must be examined very carefully [96]. Similarly to the present study, in a publication where RCA was examined with the addition of para-wood ash, the following microstructural findings were reported: SEM analyses revealed a less porous structure; EDX analyses highlighted the importance of the ratio of silicon and calcium sources, with the added ash enabling more effective utilization of these sources. As a result, the ash used enhanced pozzolanic reactions, filled micro-pores, and provided a more homogeneous microstructure. It was also found to contribute to the denser formation of C–S–H and other hydration products [97].

3.4. CBR Test Results of Waste-Enhanced RCA and BA Mixture

In the tests conducted with 35% RCA without any additional additives, the samples did not fully meet the 120% CBR requirement specified in the KTŞ standards but achieved a close value of 113%. Subsequently, SSA and CCS were added to the BA and RCA mixture, and the samples underwent 7- and 14-day curing, followed by 4 days of soaking. The results obtained from these tests are presented in Figure 13. This analysis allowed for the evaluation of the impact of SSA and CCS on CBR values, demonstrating their effectiveness in enhancing the mixture's performance.

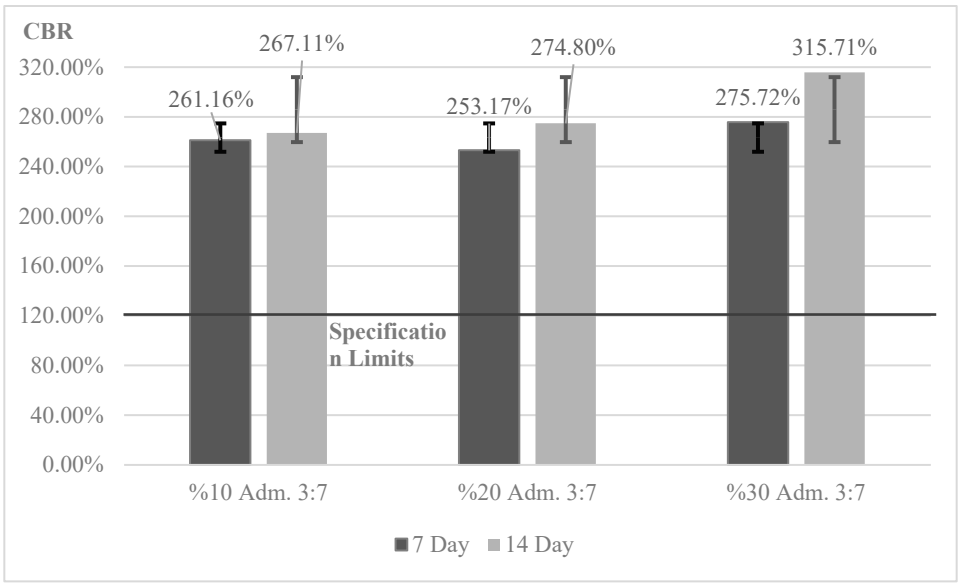


Figure 13. Soaked CBR results for SSA- and CCS-enhanced mixtures (mean ± SD, n = 2).

The results indicate that all modified samples met the KTŞ requirements after 7 and 14 days of curing, with values at least twice as high as the required limits. Additionally, in parallel with the UCS test findings, the optimal result was achieved with 30% additive content and a 3:7 SSA/CCS ratio at 14 days of curing. Furthermore, it was observed that increased additive content led to higher CBR values at 14 days. According to the literature, materials such as SSA and CCS contribute to filling voids through pozzolanic slurry, enhancing the strength and durability of the mixture [97]. This explains the observed increase in CBR values after the curing period in all samples. The pozzolanic reaction products fill the pores and reduce permeability, improving load distribution and stiffness.

3.5. Cyclic Plate Loading Test Results

Upon analyzing the cyclic plate loading test results, the load duration vs. displacement graph is presented in Figure 14.

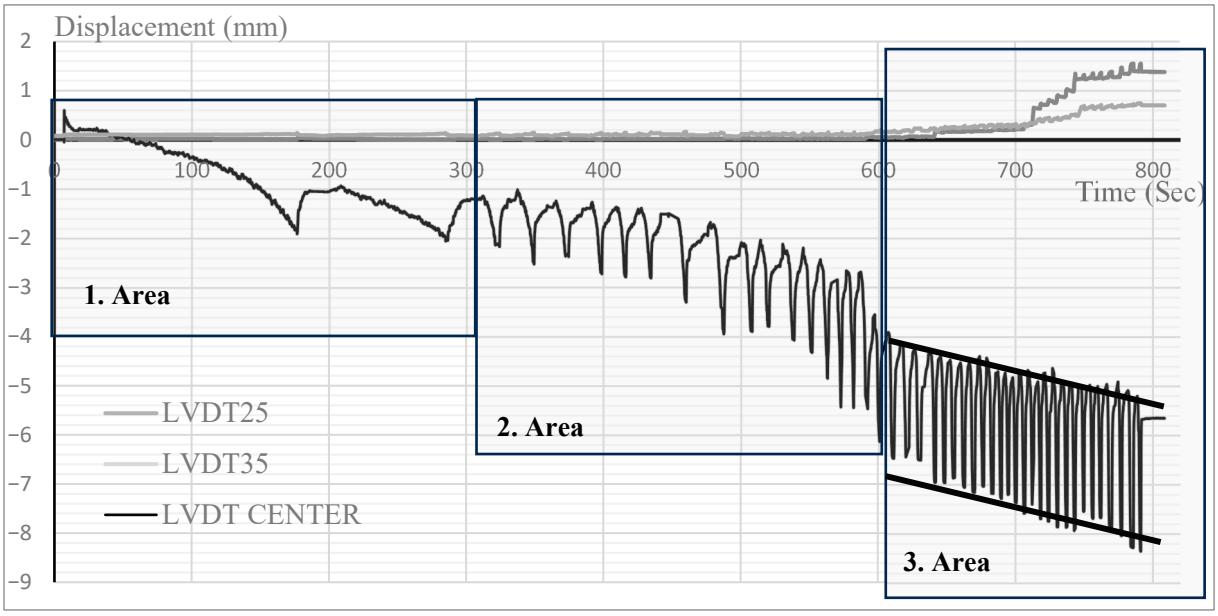


Figure 14. Recoverable displacement (δr) is evaluated as the rebound within a loading–unloading cycle, while permanent deformation corresponds to the residual settlement after unloading.

Figure 14 presents the displacement history recorded during the cyclic plate loading test. In cyclic loading, the total vertical displacement can be decomposed into a recoverable (elastic) component and a permanent (plastic) component. Here, the recoverable displacement, δr, is taken as the rebound within each cycle (difference between peak displacement at maximum load and the displacement after unloading), whereas the permanent deformation corresponds to the residual settlement accumulated after unloading [82,83]. As observed in Figure 14, the recoverable displacement remained approximately constant ($\delta r \approx 2.5$ mm), and the incremental permanent deformation became negligible towards the end of the test, indicating a stabilized response under the applied loading level.

To provide an engineering-relevant stiffness indicator commonly derived from plate tests, an equivalent modulus of subgrade reaction (surface stiffness) was estimated as the ratio of the mean contact stress under the plate to the recoverable displacement. Using a 30 cm diameter rigid plate and a peak load of 35 kN, the mean contact stress is approximately 0.50 MPa, resulting in an equivalent stiffness on the order of 0.20 GN/m^3 based on $\delta r \approx 2.5$ mm. This value is reported as an indicative stiffness parameter derived from the applied loading level and rebound displacement [84,85].

The tensile and compressive strain readings recorded in the base layer ($\varepsilon t \approx 60 \times 10^{-6}$ and $\varepsilon c \approx 110 \times 10^{-6}$) are lower than some values reported in the literature for different pavement configurations and loading conditions (Figure 15). However, because plate diameter, applied stress level, layer system (e.g., asphalt presence), boundary conditions, and instrumentation differ between studies, the comparison is considered qualitative and is provided only for order-of-magnitude context [84,85]. There are numerous studies in the literature related to this topic. When comparing the strain values found in the literature with the strain values of the plantmix base designed in this study, it is evident that the strain values in this study are significantly lower. This indicates that in pavement design, both failure resistance and rutting performance will allow for a significantly higher number of load repetitions [86–88,91].

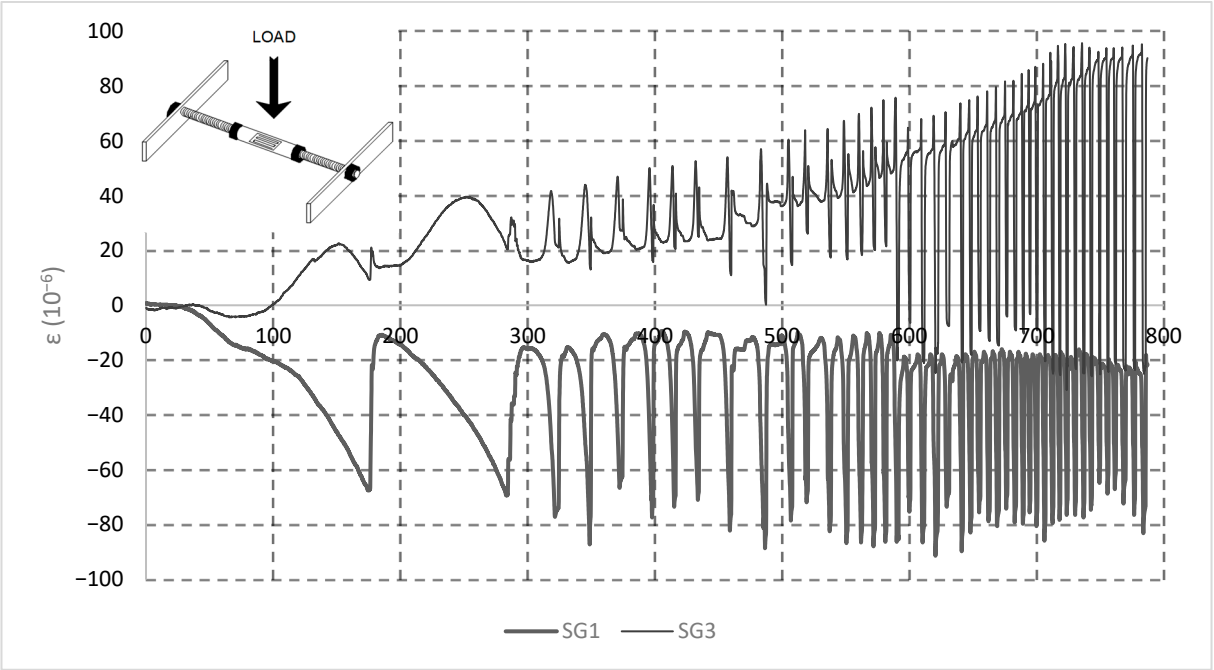


Figure 15. Strain value–cyclic load graph.

4. Conclusions

In this study, recycled concrete aggregate (RCA) was used both as a fine aggregate and in combination with other waste-based additives to enhance its performance. All modified samples achieved at least double the CBR values compared to untreated ones, demonstrating the effectiveness of the proposed mixture design. The results identified an optimal RCA content of 35% by weight, as higher ratios caused inconsistencies in CBR performance.

Unconfined compressive strength (UCS) tests showed that a 3:7 ratio of calcium carbide sludge (CCS) to sewage sludge ash (SSA) produced the highest strength. SSA played a key role in accelerating pozzolanic reactions, and the 3:7 ratio provided a balanced chemical environment that enhanced pore filling and the formation of additional binding gels. These synergistic effects explain the superior UCS and CBR values observed in this mixture.

UCS testing also proved to be a practical method for optimizing mixture design. When CBR tests were later performed on samples prepared according to UCS-based ratios, consistently high CBR values were obtained. Therefore, UCS testing can serve as a reliable preliminary screening tool to minimize the need for resource-intensive CBR testing.

The plantmix base prepared with 35% RCA, enhanced with CCS and SSA, achieved an outstanding CBR value of approximately 315%. Under a 35 kN cyclic plate loading test, only a 2.5 mm recoverable displacement and a vertical compressive strain of 110×10^{-6} were observed, confirming the mixture's superior load-bearing capacity and its suitability for high-fatigue, rut-resistant pavement structures. However, the cyclic plate loading program employed a limited number of cycles and a stabilization-based stopping criterion (constant displacement difference over 50 cycles). Accordingly, the reported cyclic response should be interpreted as an initial verification of deformation and strain stabilization. Further work is recommended to evaluate long-term fatigue and rutting performance using a substantially larger number of cycles and representative load spectra.

From an economic perspective, the construction sector consumes 40% of global energy and generates 50% of total waste, making waste reuse essential. Based on 2024 cost data from the Turkish General Directorate of Highways, aggregate procurement and transportation account for over 93% of the total cost of road base construction. Using 35% RCA

significantly reduces aggregate-related expenses, while sourcing RCA from urban demolition sites shortens transportation distances and minimizes costs. Additionally, the reuse of RCA, CCS, and SSA mitigates waste storage issues, offering a more sustainable and cost-effective alternative for infrastructure development. Studies in the literature indicate that aggregate production costs are approximately 20% for drilling and blasting, 45% for crushing and screening, and 35% for loading and transportation. Even considering these costs, it is clear that RCA use would result in at least 50% lower costs [98].

The findings are particularly applicable to Yalova Province, where extensive urban transformation is underway and over 6000 high-risk buildings have been identified. The region's valuable agricultural land, limited local stone resources, and high transportation costs make the proposed mixture design highly advantageous. Furthermore, incorporating local industrial by-products—such as CCS waste from shipyards—reduces environmental pressures while supporting a circular economy approach.

The proposed mixture design aligns closely with the United Nations Sustainable Development Goals (SDGs). It promotes sustainable urban transformation (SDG 11), reduces dependence on natural aggregates and supports circular resource use (SDG 12), lowers carbon emissions by substituting cement and lime with industrial by-products (SDG 13), and introduces innovative infrastructure solutions (SDG 9) by converting waste into valuable construction materials.

Finally, the mechanical assessment in this study is based on compaction characteristics, soaked CBR, UCS, and a small-scale cyclic plate loading verification. While CBR is widely used as an index test to evaluate the potential strength of subgrade/subbase/base materials, mechanistic–empirical pavement design frameworks typically require resilient modulus (Mr) and permanent deformation parameters for unbound layers. Therefore, future work should include resilient modulus testing and long-term rutting/permanent deformation evaluation under representative stress states and load repetitions. Another limitation is that inferential statistical analyses (e.g., ANOVA or nonparametric equivalents) were not performed, primarily because a limited number of laboratory tests were conducted with a limited number of repetitions due to material and labor intensity. Consequently, the differences observed between mixtures were discussed in comparison with results in the literature; future studies should perform the new experiments mentioned above, increase the number of repetitions to statistically validate mixture differences, and report appropriate inferential statistics (*p*-values and/or confidence intervals). In addition, the sustainability discussion in this paper is qualitative and focuses on waste diversion and reduced virgin aggregate demand; a full life cycle assessment conducted in accordance with ISO 14040/14044 is recommended to quantify environmental impacts.

Funding: This study was supported by the Yalova University Scientific Research Project (Project Code: 2024/ÖNAP/0009).

Institutional Review Board Statement: Not applicable.

Informed Consent Statement: Not applicable.

Data Availability Statement: The raw data supporting the conclusions of this article will be made available by the author on request.

Conflicts of Interest: The author declares no conflicts of interest.

Abbreviations

The following abbreviations are used in this manuscript:

RCA	Recycled Concrete Aggregate
CCS	Calcium Carbide Slag

SSA	Sewage Sludge Ash
CBR	California Bearing Ratio
BA	Basalt Aggregate
UCS	Unconfined Compressive Strength
KTŞ	Highway Technical Specification of Türkiye

References

1. Aytekin, B. Investigation of the Usability of Recycled Concrete Aggregates in Road Base and Subbase Layers. Ph.D. Thesis, Bursa Uludağ University, Bursa, Türkiye, 2021.
2. Doğdu, G.; Alkan, S.N. Deprem sonrası oluşan inşaat ve yıkıntı atıklarının değerlendirilmesi: 6 Şubat 2023 Kahramanmaraş depremleri. *Artvin Çoruh Üniv. Müh. Fen Bilim. Derg.* **2023**, *1*, 38–50.
3. Bahşi, E.; Dada, A.; Gümüş, E.; Cenikli, S. Evaluation of numerical analysis results of buildings identified as risky under Law No. 6306. *Resilience* **2023**, *7*, 153–169. [CrossRef]
4. Tunc, A. The importance of building inventory update in urban regeneration of Turkey: A call for action and solution. *Glob. J. Ecol.* **2024**, *9*, 001–010. [CrossRef]
5. Li, W.; Yi, Y.; Puppala, A.J. Utilization of carbide slag-activated ground granulated blastfurnace slag to treat gypseous soil. *Soils Found.* **2019**, *59*, 1496–1507. [CrossRef]
6. Duan, H.; Miller, T.R.; Liu, G.; Tam, V.W. Construction debris becomes growing concern of growing cities. *Waste Manag.* **2019**, *83*, 1–5. [CrossRef]
7. Güllü, G. Kentsel dönüşümde sıfır atık yönetimi. *İstanb. Sabahattin Zaim Üniv. Fen Bilim. Enst. Derg.* **2022**, *4*, 112–120. [CrossRef]
8. Ahmed, W.; Ye, C.; Lu, G.; Ng, S.T.; Liu, G.; Wang, Y. Low-carbon concrete comprising high-volume pozzolan and recycled aggregate: Evaluating mechanical performance, microstructure, environmental impact, and cost efficiency. *J. Clean. Prod.* **2025**, *518*, 145796. [CrossRef]
9. Oikonomou, N.D. Recycled concrete aggregates. *Cem. Concr. Compos.* **2005**, *27*, 315–318. [CrossRef]
10. Silva, R.V.; Jiménez, J.R.; Agrela, F.; de Brito, J. Real-scale applications of recycled aggregate concrete. In *New Trends in Eco-Efficient and Recycled Concrete*; Woodhead Publishing: Cambridge, UK, 2019; pp. 573–589. [CrossRef]
11. Arulrajah, A.; Piratheepan, J.; Ali, M.M.; Bo, M.W. Geotechnical properties of recycled concrete aggregate in pavement subbase applications. *Geotech. Test. J.* **2012**, *35*, 743–751. [CrossRef]
12. Poltue, T.; Suddeepong, A.; Horpibulsuk, S.; Samingthong, W.; Arulrajah, A.; Rashid, A.S.A. Strength development of recycled concrete aggregate stabilized with fly ash-rice husk ash based geopolymer as pavement base material. *Road Mater. Pavement Des.* **2020**, *21*, 2344–2355. [CrossRef]
13. Tabyang, W.; Suksiripattanapong, C.; Phetchuay, C.; Laksanakit, C.; Chusilp, N. Evaluation of municipal solid waste incineration fly ash-based geopolymer for stabilised recycled concrete aggregate as road material. *Road Mater. Pavement Des.* **2022**, *23*, 2178–2189. [CrossRef]
14. Arulrajah, A.; Mohammadinia, A.; Phummiphan, I.; Horpibulsuk, S.; Samingthong, W. Stabilization of recycled demolition aggregates by geopolymers comprising calcium carbide residue, fly ash and slag precursors. *Constr. Build. Mater.* **2016**, *114*, 864–873. [CrossRef]
15. Chompoorat, T.; Thepumong, T.; Khamplod, A.; Likitlersuang, S. Improving mechanical properties and shrinkage cracking characteristics of soft clay in deep soil mixing. *Constr. Build. Mater.* **2022**, *316*, 125858. [CrossRef]
16. Wang, J.; Fan, Y.; Xiong, X.; Zhao, F. Stabilization of shield muck treated with calcium carbide slag–fly ash. *Buildings* **2023**, *13*, 1707. [CrossRef]
17. Xue, X.; Gao, J.; Hu, K. Performance evaluation of cement stabilized mixture with recycled aggregate from construction and demolition waste. *Iran. J. Sci. Technol. Trans. Civ. Eng.* **2021**, *46*, 3093–3106. [CrossRef]
18. Pérez, P.; Agrela, F.; Herrador, R.; Ordoñez, J. Application of cement-treated recycled materials in the construction of a section of road in Malaga, Spain. *Constr. Build. Mater.* **2013**, *44*, 593–599. [CrossRef]
19. Mishra, U.C.; Sarsaiya, S.; Gupta, A. A systematic review on the impact of cement industries on the natural environment. *Environ. Sci. Pollut. Res.* **2022**, *29*, 18440–18451. [CrossRef] [PubMed]
20. Mohamad, N.; Muthusamy, K.; Embong, R.; Kusbiantoro, A.; Hashim, M.H. Environmental impact of cement production and solutions: A review. *Mater. Today Proc.* **2022**, *48*, 741–746. [CrossRef]
21. Zulfiqar, Q.; Haider, S.W.; Cetin, B.; Coban, H.S.; Abdollahi, S.F. Comparison of lab versus backcalculated moduli of virgin aggregate and recycled aggregate base layers. *Appl. Sci.* **2024**, *14*, 9049. [CrossRef]
22. Kavussi, A.; Hassani, A.; Kazemian, F.; Taghipoor, M. Laboratory evaluation of treated recycled concrete aggregate in asphalt mixtures. *Int. J. Pavement Res. Technol.* **2019**, *12*, 26–32. [CrossRef]

23. Nwakaire, C.M.; Onn, C.C.; Yap, S.P.; Yuen, C.W.; Koting, S.; Mo, K.H.; Othman, F. The strength and environmental performance of asphalt mixtures with recycled concrete aggregates. *Transp. Res. Part D Transp. Environ.* **2021**, *100*, 103065. [CrossRef]
24. Singh, S.; Sharma, S.K.; Akbar, M.A. Developing zero carbon emission pavements with geopolymer concrete: A comprehensive review. *Transp. Res. Part D Transp. Environ.* **2022**, *110*, 103436. [CrossRef]
25. Horpibulsuk, S.; Phetchuay, C.; Chinkulkijniwat, A. Soil stabilization by calcium carbide residue and fly ash. *J. Mater. Civ. Eng.* **2012**, *24*, 184–193. [CrossRef]
26. Phoo-ngernkham, T.; Phiangphimai, C.; Intarabut, D.; Hanjitsuwan, S.; Damrongwiriyanupap, N.; Li, L.Y.; Chindaprasirt, P. Low cost and sustainable repair material made from alkali-activated high-calcium fly ash with calcium carbide residue. *Constr. Build. Mater.* **2020**, *247*, 118543. [CrossRef]
27. Eskisar, T. The role of carbide lime and fly ash blends on the geotechnical properties of clay soils. *Bull. Eng. Geol. Environ.* **2021**, *80*, 6343–6357. [CrossRef]
28. Jaturapitakkul, C.; Roongreung, B. Cementing material from calcium carbide residue-rice husk ash. *J. Mater. Civ. Eng.* **2003**, *15*, 470–475. [CrossRef]
29. Julphunthong, P.; Joyklad, P.; Manprom, P.; Chompoorat, T.; Palou, M.T.; Suriwong, T. Evaluation of calcium carbide residue and fly ash as sustainable binders for environmentally friendly loess soil stabilization. *Sci. Rep.* **2024**, *14*, 671. [CrossRef]
30. Ge, X.; Gu, X.; Song, G.; Liu, J.; Wang, S.; Hu, Z.; Wang, X.; Hu, Z.; Wang, H. Comprehensive evaluation of low-carbon cementitious materials prepared with industrial by-product calcium carbide residue as alkali source. *Environ. Res.* **2025**, *270*, 120964. [CrossRef]
31. Li, Y.M.; Wei, W.M.; Hao, J.; Gao, P.F.; Liu, P.F.; Li, G.N.; Yang, F.-H.; Wang, Z.J. Demonstration application of Chinese-made chlorine bypass system for stable cement kiln using calcium carbide residue as main raw material. *J. Mater. Cycles Waste Manag.* **2022**, *24*, 618–632. [CrossRef]
32. Bawab, J.; El-Hassan, H.; El-Dieb, A.; Khatib, J.; El-Mir, A. Utilization of calcium carbide residue as a concrete component: A comprehensive review. *Case Stud. Constr. Mater.* **2025**, *22*, e04823. [CrossRef]
33. İpek, M. Effects of Compaction Pressure Applied during Setting on the Mechanical Behavior of Reactive Powder Concrete. Ph.D. Thesis, Sakarya University, Sakarya, Türkiye, 2009.
34. Hasan, S.S.; Fattah, M.Y. Strength properties of polymer reactive powder concrete with waste materials. *Civ. Eng. J.* **2023**, *9*, 1936–1956. [CrossRef]
35. Mao, X.; Qu, W.; Zhu, P. Mixture optimization of green reactive powder concrete with recycled powder. *J. Mater. Civ. Eng.* **2019**, *31*, 04019033. [CrossRef]
36. Liu, S.; Wang, D.; Guo, J.; Zhang, L.; Yuan, N. Pressed recycled fly ash and carbide slag: Hydration of entirely waste-stream building components. *Constr. Build. Mater.* **2020**, *265*, 120282. [CrossRef]
37. Yunsheng, Z.; Wei, S.; Sifeng, L.; Chujie, J.; Jianzhong, L. Preparation of C200 green reactive powder concrete and its static–dynamic behaviors. *Cem. Concr. Compos.* **2008**, *30*, 831–838. [CrossRef]
38. Salim, L.G.; Al-Baghdadi, H.M.; Muteb, H.H. Reactive powder concrete with steel, glass and polypropylene fibers as a repair material. *Civil Eng. J.* **2019**, *5*, 2441–2449. [CrossRef]
39. Liu, J.C.; Ji, H.; Kwan, A.K.H.; Ye, H. Optimization of alkali-activated binder reactive powder concrete based on concept of packing density. *Powder Technol.* **2024**, *440*, 119778. [CrossRef]
40. Guo, W.; Zhang, Z.; Zhao, Q.; Song, R.; Liu, J. Mechanical properties and microstructure of binding material using slag-fly ash synergistically activated by wet-basis soda residue-carbide slag. *Constr. Build. Mater.* **2021**, *269*, 121301. [CrossRef]
41. Gong, X.; Zhang, T.; Zhang, J.; Wang, Z.; Liu, J.; Cao, J.; Wang, C. Recycling and utilization of calcium carbide slag: Current status and new opportunities. *Renew. Sustain. Energy Rev.* **2022**, *159*, 112133. [CrossRef]
42. Kahraman, S. Improvement and Comparative Analysis of Clay Soils Using Calcium Carbide Waste. Master's Thesis, Karabük University, Karabük, Türkiye, 2020.
43. Chen, S.; Yuan, H. Characterization and optimization of eco-friendly cementitious materials based on titanium gypsum, fly ash, and calcium carbide residue. *Constr. Build. Mater.* **2022**, *349*, 128635. [CrossRef]
44. Ma, X.; Yang, Y. Single-Component Low-Carbon Sustainable Geopolymer Synthesis Using Calcium Carbide Residue, Gypsum, Sewage Sludge Ash, and Ground Granulated Blast Slag. *Sustain. Mater. Technol.* **2025**, *43*, e01314. [CrossRef]
45. Akpaki, O.; Toi Bissang, B.; Megnassan, S.; Baba, G. Calcium carbide treatment of faecal sludge. *J. Mater. Environ. Sci.* **2023**, *14*, 1187–1195.
46. Qarani, A.S.; Sabah, M.J. Wastewater sludge characteristics, treatment techniques and energy production. *Recycl. Sustain. Dev.* **2022**, *15*, 9–26. [CrossRef]
47. Kaza, S.; Yao, L.; Bhada-Tata, P.; Van Woerden, F. *What a Waste 2.0: A Global Snapshot of Solid Waste Management to 2050*; World Bank Publications: Washington, DC, USA, 2018.
48. Karadurmuş, U.; Sarı, M. Marine mucilage in the Sea of Marmara and its effects on the marine ecosystem: Mass deaths. *Turk. J. Zool.* **2022**, *46*, 93–102. [CrossRef]

49. Koncagül, M.; Dülger, N.E.; Yinanç, A. Dünyada ve Marmara Denizi'nde müsilaj oluşumu ve etkileri. *Eur. J. Eng. Appl. Sci.* **2022**, *5*, 73–79. [CrossRef]
50. Melikoglu, M. Forecasting of municipal solid waste generation in Türkiye and techno-economic-environmental assessment of electricity generation via incineration till 2032. *Next Sustain.* **2025**, *5*, 100092. [CrossRef]
51. Chen, B.; Perumal, P.; Illikainen, M.; Ye, G. A review on the utilization of municipal solid waste incineration bottom ash as a mineral resource for construction materials. *J. Build. Eng.* **2023**, *71*, 106386. [CrossRef]
52. Seferoğlu, A.G. Performance Evaluation of Cement-Treated Reclaimed Asphalt Pavement Bases Under Repeated Loading and Cost Analysis. Ph.D. Thesis, Karadeniz Technical University, Trabzon, Türkiye, 2017.
53. Gray, J.E. *Characteristics of Graded Base Course Aggregates Determined by Triaxial Tests*; Engineering Bulletin No. 12; National Crushed Stone Association: Washington, DC, USA, 1962.
54. Barksdale, R.D.; Itani, S.Y. Influence of aggregate shape on base behavior. *Transp. Res. Rec.* **1989**, *1227*, 173–182.
55. Huang, Y.H.; Rose, J.G.; Khoury, C.J. Design and performance of flexible pavements. *Transp. Res. Rec.* **1986**, *1095*, 102–110.
56. Cai, Y.; Zang, Z.; Zuo, X.; Liu, F.; Li, L.; Lu, K.; Huang, Q. Research on the performance of calcium carbide slag–fly ash stabilized soil. *Adv. Civ. Eng.* **2023**, *2023*, 4571162. [CrossRef]
57. Highway General Directorate (KGM). *Highway Technical Specifications*; Ministry of Transportation and Infrastructure: Ankara, Turkey, 2023.
58. Pacana, A.; Siwiec, D.; Bednarova, L.; Sofranko, M.; Vegsoova, O.; Cvoliga, M. Influence of natural aggregate crushing process on crushing strength index. *Sustainability* **2021**, *13*, 8353. [CrossRef]
59. Singh, R.; Nayak, D.; Pandey, A.; Kumar, R.; Kumar, V. Effects of recycled fine aggregates on properties of concrete containing natural or recycled coarse aggregates: A comparative study. *J. Build. Eng.* **2022**, *45*, 103442. [CrossRef]
60. Prasad, D.; Pandey, A.; Kumar, B. Sustainable production of recycled concrete aggregates by lime treatment and mechanical abrasion for M40 grade concrete. *Constr. Build. Mater.* **2021**, *268*, 121119. [CrossRef]
61. Guedes, M.; Evangelista, L.; de Brito, J.; Ferro, A.C. Microstructural characterization of concrete prepared with recycled aggregates. *Microsc. Microanal.* **2013**, *19*, 1222–1230. [CrossRef]
62. Choeycharoen, P.; Sornlar, W.; Wannagon, A. A Sustainable bottom ash-based alkali-activated materials and geopolymers synthesized by using activator solutions from industrial wastes. *J. Build. Eng.* **2022**, *54*, 104659. [CrossRef]
63. Baeza-Brotons, F.; Garcés, P.; Payá, J.; Saval, J.M. Portland cement systems with addition of sewage sludge ash. Application in concretes for the manufacture of blocks. *J. Clean. Prod.* **2014**, *82*, 112–124. [CrossRef]
64. Nakic, D. Environmental evaluation of concrete with sewage sludge ash based on LCA. *Sustain. Prod. Consum.* **2018**, *16*, 193–201. [CrossRef]
65. Azarhomayun, F.; Haji, M.; Kioumarsi, M.; Kheyroddin, A. Combined Use of Sewage Sludge Ash and Silica Fume in Concrete. *Int. J. Concr. Struct. Mater.* **2023**, *17*, 34. [CrossRef]
66. Azed, M.A.; Ing, D.S. Properties of concrete containing microwaved sewage sludge ash. *J. Mech. Eng. Sci.* **2021**, *15*, 8469–8479. [CrossRef]
67. Zabielska-Adamska, K. Sewage Sludge Bottom Ash Characteristics and Potential Application in Road Embankment. *Sustainability* **2020**, *12*, 39. [CrossRef]
68. *ASTM C618-19*; Standard Specification for Coal Fly Ash and Raw or Calcined Natural Pozzolan for Use in Concrete. ASTM International: West Conshohocken, PA, USA, 2019.
69. Navruz, H.Ö.; Aykan, M.; Çömez, Ş.; Komut, M. *Toprak ve Stabilizasyon Laboratuvarı El Kitabı; Karayolları Genel Müdürlüğü*; Ulaştırma ve Altyapı Bakanlığı: Ankara, Türkiye, 2021.
70. *ASTM D1883-21*; Standard Test Method for California Bearing Ratio (CBR) of Laboratory Compacted Soils. ASTM International: West Conshohocken, PA, USA, 2021.
71. *ASTM D1557-09*; Standard Test Methods for Laboratory Compaction Characteristics of Soil Using Modified Effort. ASTM International: West Conshohocken, PA, USA, 2009.
72. *ASTM D698-21*; Standard Test Methods for Laboratory Compaction Characteristics of Soil Using Standard Effort. ASTM International: West Conshohocken, PA, USA, 2021.
73. *AASHTO T 180*; Standard Method of Test for Moisture–Density Relations of Soils Using a 4.54-kg (10-lb) Rammer and a 457-mm (18 in.) Drop. American Association of State Highway and Transportation Officials: Washington, DC, USA, 2022.
74. Qian, Y.; Han, J.; Pokharel, S.K.; Parsons, R.L. Experimental study on triaxial geogrid-reinforced bases over weak subgrade under cyclic loading. In Proceedings of the GeoFlorida 2010, West Palm Beach, FL, USA, 20–24 February 2010. [CrossRef]
75. O'Flaherty, C.A.; David, H.T.; Davidson, D.T. Relationship between the California bearing ratio and the unconfined compressive strength of sand–cement mixtures. *Proc. Iowa Acad. Sci.* **1961**, *68*, 341–356.
76. Fu, H.; Xue, C.; Wen, W.; Yang, Q.; Chen, L. Research on the road performance of carbonaceous mudstone soil-rock mixtures under multifactor influence. *KSCE J. Civ. Eng.* **2024**, *28*, 1227–1237. [CrossRef]

77. Cook, J.R.; Gourley, C.S. A framework for the appropriate use of marginal materials. In Proceedings of the World Road Association (PIARC)-Technical Committee c12 Seminar, Ulaanbaatar, Mongolia, 18–21 June 2002.
78. McCarthy, M.J.; Yakub, H.I.; Csetenyi, L.J. Impact of fly ash production and sourcing changes on chemical and physical aspects of concrete durability. *Constr. Build. Mater.* **2022**, *342*, 127313. [CrossRef]
79. Kumar, G.S.; Shankar, S. Strength and durability characteristics of lime fly ash-stabilized recycled concrete aggregate for use in low-volume rural roads. *Indian Geotech. J.* **2023**, *53*, 78–92. [CrossRef]
80. *ASTM D1195/D1195M-21*; Standard Test Method for Repetitive Static Plate Tests of Soils and Flexible Pavement Components. ASTM International: West Conshohocken, PA, USA, 2021.
81. Deutsches Institut für Normung (DIN). *Soil—Testing Procedures and Testing Equipment—Plate Load Test (DIN 18134:2012-04)*; Beuth Verlag: Berlin, Germany, 2012.
82. Seferoğlu, A.G.; Seferoğlu, M.T.; Akpinar, M.V. Experimental study on cement-treated and untreated RAP blended bases: Cyclic plate loading test. *Constr. Build. Mater.* **2018**, *182*, 580–587. [CrossRef]
83. Demir, A.; Ok, B.; Sarici, T. Evaluation of granular fill layer underlain by soft clay soil using large-scale cyclic plate loading tests. *Int. J. Civ. Eng.* **2023**, *21*, 1853–1865. [CrossRef]
84. Ekwulo, E.O.; Eme, D.B. Fatigue and rutting strain analysis of flexible pavements designed using CBR methods. *Afr. J. Environ. Sci. Technol.* **2014**, *3*, 412–421.
85. Behiry, A.E.A.E.M. Fatigue and rutting lives in flexible pavement. *Ain Shams Eng. J.* **2012**, *3*, 367–374. [CrossRef]
86. Po, Y.M.; Tsai, K.L.; Pan, E.; Lin, C.P.; Nirwal, S. Fatigue and rutting life design of layered flexible pavements via Advanced MultiSmart3D. *Int. J. Pavement Res. Technol.* **2024**, 1–13. [CrossRef]
87. Beninca, G.P.; Goulart, A. Fatigue cracking prediction of cobblestone interlayer pavement using non-destructive testing and mechanistic-empirical analyses. *Transportes* **2024**, *32*, e3022. [CrossRef]
88. Qian, Y.; Han, J.; Pokharel, S.K.; Parsons, R.L. Determination of resilient modulus of subgrade using cyclic plate loading tests. In Proceedings of the Geo-Frontiers 2011: Advances in Geotechnical Engineering, Dallas, TX, USA, 13–16 March 2011; pp. 4743–4751. [CrossRef]
89. Pokharel, S.K.; Han, J.; Leshchinsky, D.; Parsons, R.L.; Halahmi, I. Investigation of factors influencing behavior of single geocell-reinforced bases under static loading. *Geotext. Geomembr.* **2010**, *28*, 570–578. [CrossRef]
90. Thakur, J.K.; Han, J.; Parsons, R.L. Factors influencing deformations of geocell-reinforced recycled asphalt pavement bases under cyclic loading. *J. Mater. Civ. Eng.* **2017**, *29*, 04016240. [CrossRef]
91. Seferoğlu, M.T.; Acı, E.N. Chrome waste utilization in base layers: Mechanical strength and environmental risk assessment. *Case Stud. Constr. Mater.* **2025**, *22*, e04873. [CrossRef]
92. Özcanan, S.; Akpınar, M.V. Esnek üstyapılarda kritik tekerlek ve aks konfigürasyonların mekanistik analizlere göre tespit edilmesi. *Teknik Dergi* **2014**, *25*, 6625–6654.
93. Yılmaz, A. Engineering properties of basalt aggregates in terms of use in granular layers of flexible pavements. *Case Stud. Constr. Mater.* **2022**, *17*, e01182. [CrossRef]
94. Sapkota, K.; Yaghoubi, E.; Wasantha, P.L.P.; Van Staden, R.; Fragomeni, S. Mechanical characteristics and durability of HMA made of recycled aggregates. *Sustainability* **2023**, *15*, 5594. [CrossRef]
95. Adamu, M.; Ibrahim, Y.E.; Al-Atroush, M.E.; Alanazi, H. Mechanical properties and durability performance of concrete containing calcium carbide residue and nano silica. *Materials* **2021**, *14*, 6960. [CrossRef]
96. Yang, J.; Zhang, Y.; He, X.; Su, Y.; Tan, H.; Ma, M.; Strnadel, B. Heat-cured cement-based composites with wet-grinded fly ash and carbide slag slurry: Hydration, compressive strength and carbonation. *Constr. Build. Mater.* **2021**, *307*, 124916. [CrossRef]
97. Sae-Long, W.; Chompoorat, T.; Limkatanyu, S.; Damrongwiriyanupap, N.; Sukontasukkul, P.; Chub-Uppakarn, T.; Thepumong, T. Experimental and simulation analysis of RCA and para-wood ash as partial substitutes for NCA and cement in recycled aggregate concrete. *Case Stud. Constr. Mater.* **2024**, *21*, e03716. [CrossRef]
98. Fägerlind, J. Cost Analysis for Crushing and Screening-Part II: Development of a Cost Model for Determination of the Production Cost for Product Fractions. Master's Thesis, Lund University, Lund, Sweden, 2015. Available online: https://lup.lub.lu.se/student-papers/record/7851295/file/7851311.pdf (accessed on 12 January 2026).

Disclaimer/Publisher's Note: The statements, opinions and data contained in all publications are solely those of the individual author(s) and contributor(s) and not of MDPI and/or the editor(s). MDPI and/or the editor(s) disclaim responsibility for any injury to people or property resulting from any ideas, methods, instructions or products referred to in the content.